Retrieval of all effective susceptibilities in nonlinear metamaterials

Stéphane Larouche* and Vesna Radisic
NG Next, Northrop Grumman Corporation, Redondo Beach, California 90278, USA

(Received 24 October 2017; published 30 April 2018)

Electromagnetic metamaterials offer a great avenue to engineer and amplify the nonlinear response of materials. Their electric, magnetic, and magnetoelectric linear and nonlinear response are related to their structure, providing unprecedented liberty to control those properties. Both the linear and the nonlinear properties of metamaterials are typically anisotropic. While the methods to retrieve the effective linear properties are well established, existing nonlinear retrieval methods have serious limitations. In this work, we generalize a nonlinear transfer matrix approach to account for all nonlinear susceptibility terms and show how to use this approach to retrieve all effective nonlinear susceptibilities of metamaterial elements. The approach is demonstrated using sum frequency generation, but can be applied to other second-order or higher-order processes.

DOI: 10.1103/PhysRevA.97.043863

I. INTRODUCTION

Nonlinear metamaterials offer unprecedented control over the nonlinear properties of materials, as well as access to new exotic properties not available in standard materials [1]. It has been proposed that they will play a significant role for new devices operating over a wide range of the electromagnetic spectrum [2,3].

The advantage of metamaterials over other structured materials is the possibility to assign them effective properties, i.e., the properties of a homogeneous effective material producing the same effect as the metamaterial. This is a powerful concept allowing one to separate the design of the metamaterial unit cell from that of the device where the metamaterial is used. The latter would be prohibitively difficult, if it were even possible, if one needed to consider all the details of the structure of every unit cell.

The retrieval of metamaterial effective linear properties is well established [4–6]. Some approaches for the retrieval of effective nonlinear properties of metamaterials have also been proposed [7–11], but they are limited to metamaterials with enough symmetry (such as isotropic metamaterials) that it is possible to treat the elements of the nonlinear susceptibility tensors separately. Many nonlinear metamaterials do not respect this assumption and it is necessary to generalize the nonlinear retrieval approach to account for all nonlinear susceptibilities at once [12].

In this paper, we present a general retrieval approach for nonlinear metamaterials. The idea behind the retrieval approach, like for its linear counterpart, is to find the properties of a uniform slab of material producing the same effect as a slab of metamaterial. We therefore show how to calculate the waves generated by a slab of general bianisotropic nonlinear material, and how to express the retrieval problem as the solution of a linear system of equations. In order to calculate the nonlinearly generated waves, we need to know the fields inside the bianisotropic slab. We therefore first review a transfer matrix approach for linear bianisotropic materials. Then, we extend a nonlinear transfer matrix approach to include such materials, as well as magnetic and magnetoelectric nonlinearities. Finally, we show how the nonlinear transfer matrix approach can be used to build a linear system of equations to retrieve all the nonlinear susceptibility terms.

II. TRANSFER MATRIX APPROACH FOR BIANISOTROPIC MATERIALS

Calculating the reflection and transmission of a stack of material slabs is a one-dimensional problem. For linear isotropic materials, the problem can be separated into transverse electric (TE) and transverse magnetic (TM) waves. Many approaches based on 2×2 matrices exist for this problem, and are often presented in electromagnetics and optics textbooks, such as that of Born and Wolf [13]. In the case of anisotropic, magnetoelectric, or bianisotropic materials, it is impossible to separate the problem into TE and TM waves. In this case, 4×4 matrix approaches can be used [14,15]; in this paper, we use the approach of Berreman [14]. As this approach is not widely used, and it is necessary to understand it for the nonlinear calculations, we review it in this section. We first determine the propagation modes in a bianisotropic material. We then build transfer and scattering matrices to calculate reflection and transmission, as well as the fields at all positions in the stack.

A. Propagation modes

To calculate the propagation of a wave through a series of slabs of materials it is possible, without loss of generality, to choose the system of coordinates such that the system is uniform in the xy plane, and varies only in the z direction. In the absence of interfacial currents, the in-plane components of the electric and magnetic fields E_x, E_y, H_x, and H_y are continuous at the interfaces, making them a natural choice to express the propagation modes. Furthermore, the in-plane components of the propagation constant, k_x and k_y, are invariant through the

*stephane.larouche@northropgrummannext.net

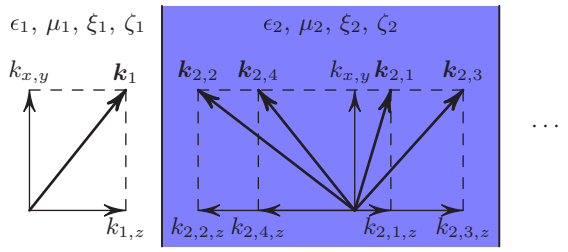

FIG. 1. The system considered consists of a series of slabs of potentially bianisotropic materials in which we need to determine the modes and their propagation constants. The propagation constant of the applied wave ($\boldsymbol{k}_1$ here) sets the in-plane propagation constants k_x and k_y (jointly indicated by $k_{x,y}$), which are invariant throughout the whole system. Inside every slab, there are four modes with potentially different propagation constants. Since k_x and k_y are invariant, only k_z varies for each mode and can be determined using the approach described in the text. In medium 2, for example, we want to determine the z component of the propagation constant of the four modes $k_{2,1,z}$, $k_{2,2,z}$, $k_{2,3,z}$, and $k_{2,4,z}$. The determination must be performed independently for each medium.

whole system. As shown in Fig. 1, our goal is to determine the propagation constant in the z direction and the associated modes.

As described in details in Appendix A, Maxwell's and material equations can be combined to create a system of six coupled equations for all components of the electric and magnetic fields. The invariance of k_x and k_y allows the elimination of two equations. Choosing to keep the in-plane components, for the reasons just described, we arrive at

$$k_z \begin{bmatrix} E_x \\ H_y \\ E_y \\ -H_x \end{bmatrix} = \Delta \begin{bmatrix} E_x \\ H_y \\ E_y \\ -H_x \end{bmatrix}, \tag{1}$$

where

$$\Delta = \omega \begin{bmatrix} 0 & 0 & 0 & 1 \\ 1 & 0 & 0 & 0 \\ 0 & 0 & -1 & 0 \\ 0 & 1 & 0 & 0 \end{bmatrix} \left(\begin{bmatrix} \epsilon_{xx} & \epsilon_{xy} & \xi_{xx} & \xi_{xy} \\ \epsilon_{yx} & \epsilon_{yy} & \xi_{yx} & \xi_{yy} \\ \zeta_{xx} & \zeta_{xy} & \mu_{xx} & \mu_{xy} \\ \zeta_{yx} & \zeta_{yy} & \mu_{yx} & \mu_{yy} \end{bmatrix} - \begin{bmatrix} \epsilon_{xz} & \xi_{xz} + \frac{k_y}{\omega} \\ \epsilon_{yz} & \xi_{yz} - \frac{k_x}{\omega} \\ \zeta_{xz} - \frac{k_y}{\omega} & \mu_{xz} \\ \zeta_{yz} + \frac{k_x}{\omega} & \mu_{yz} \end{bmatrix} \begin{bmatrix} \epsilon_{zz} & \xi_{zz} \\ \zeta_{zz} & \mu_{zz} \end{bmatrix}^{-1} \right.$$
$$\left. \times \begin{bmatrix} \epsilon_{zx} & \epsilon_{zy} & \xi_{zx} - \frac{k_y}{\omega} & \xi_{zy} + \frac{k_x}{\omega} \\ \zeta_{zx} + \frac{k_y}{\omega} & \zeta_{zy} - \frac{k_x}{\omega} & \mu_{zx} & \mu_{zy} \end{bmatrix} \right) \begin{bmatrix} 1 & 0 & 0 & 0 \\ 0 & 0 & 1 & 0 \\ 0 & 0 & 0 & -1 \\ 0 & 1 & 0 & 0 \end{bmatrix}, \tag{2}$$

while ω is the angular frequency,

$$\epsilon = \begin{bmatrix} \epsilon_{xx} & \epsilon_{xy} & \epsilon_{xz} \\ \epsilon_{yx} & \epsilon_{yy} & \epsilon_{yz} \\ \epsilon_{zx} & \epsilon_{zy} & \epsilon_{zz} \end{bmatrix} \text{ and } \epsilon = \begin{bmatrix} \mu_{xx} & \mu_{xy} & \mu_{xz} \\ \mu_{yx} & \mu_{yy} & \mu_{yz} \\ \mu_{zx} & \mu_{zy} & \mu_{zz} \end{bmatrix}$$

are the permittivity and permeability of the material, and

$$\xi = \begin{bmatrix} \xi_{xx} & \xi_{xy} & \xi_{xz} \\ \xi_{yx} & \xi_{yy} & \xi_{yz} \\ \xi_{zx} & \xi_{zy} & \xi_{zz} \end{bmatrix} \text{ and } \zeta = \begin{bmatrix} \zeta_{xx} & \zeta_{xy} & \zeta_{xz} \\ \zeta_{yx} & \zeta_{yy} & \zeta_{yz} \\ \zeta_{zx} & \zeta_{zy} & \zeta_{zz} \end{bmatrix}$$

are the magnetoelectric coupling constants.

Equation (1) is an eigenvalue equation. The propagation constants in the z direction are the eigenvalues of Δ while the propagation modes are its eigenvectors. There are four propagation modes, each with its associated propagation constant.

It is worth noting that in anisotropic materials the direction of k_z is not always the propagation direction. The latter must be determined using the Poynting vector, which can be calculated from the modes. There are always two forward and two backward propagating modes. The modes can also be grouped by polarization as there are always pairs of forward and backward propagating modes with the same polarization, such as right and left elliptically polarized.

In materials with high symmetry, the propagation constants are often degenerate. For example, in an isotropic material, all four propagation constants have the same absolute value, two of them positive and two of them negative. Furthermore, if the plane of incidence is either the xz or yz planes (which is always possible by an appropriate choice of system of coordinates), Δ is block diagonal and can be separated into a pair of 2×2 matrices for TE and TM waves.

B. Transfer matrices

In the previous section, we determined the propagation modes and constants in a uniform medium. In this section, we show how to calculate the properties of a stack of material slabs.

As mentioned in the previous section, there are four propagation modes in each slab of material. We can express the fields in a slab as a vector of the amplitudes of those four modes:

$$\boldsymbol{A} = \begin{bmatrix} A_1 \\ A_2 \\ A_3 \\ A_4 \end{bmatrix}.$$

The modes can be arranged in any order. For simplicity, let us suppose that modes 1 and 3 are forward propagating, while modes 2 and 4 are backward propagating. Let us also suppose that modes 1 and 2, as well as modes 3 and 4, are of the same polarization pairwise.

At the interface between two materials, in the absence of surface currents and charges, the tangential components of the electric and magnetic fields are continuous. To determine the tangential components at the interface, we need to sum the x and y components from the four modes using

$$\begin{bmatrix} E_x \\ H_y \\ E_y \\ -H_x \end{bmatrix} = \Pi \boldsymbol{A},$$

where Π is a matrix whose rows are the propagation modes inside of the slab (in the same order selected for $\boldsymbol{A}$). At the interface between slabs $i-1$ and i,

$$\Pi_{i-1}\boldsymbol{A}_{i-1}(z_i) = \Pi_i \boldsymbol{A}_i(z_i),$$

where z_i is the position of the interface. Therefore, the transfer matrix of the interface is

$$M_{i-1,i} = \Pi_i^{-1}\Pi_{i-1}. \tag{3}$$

Inside a uniform slab, the modes propagate without interacting and simply accumulate phase. The transfer matrix related to the propagation inside slab i is

$$\Phi_i = \begin{bmatrix} e^{ik_{z,i,1}d_i} & 0 & 0 & 0 \\ 0 & e^{ik_{z,i,2}d_i} & 0 & 0 \\ 0 & 0 & e^{ik_{z,i,3}d_i} & 0 \\ 0 & 0 & 0 & e^{ik_{z,i,4}d_i} \end{bmatrix}, \tag{4}$$

where the $k_{z,i}$'s are the eigenvalues of Δ_i and $d_i = z_{i+1} - z_i$ is the thickness of the slab.

The transfer matrix of a whole stack of slabs is obtained by multiplying the individual transfer matrices. For example, the transfer matrix of a slab of material 2 sandwiched between two semi-infinite media 1 and 3 is

$$M = M_{2,3}\Phi_2 M_{1,2}. \tag{5}$$

C. Scattering matrices (reflection and transmission)

The mode amplitudes on both sides of a stack of $n-2$ slabs are related by the transfer matrix of the system such that

$$\boldsymbol{A}_n = M\boldsymbol{A}_1. \tag{6}$$

However, in practice, it is rare that all the amplitudes on either side are known. More often, the incoming waves are known, while the outgoing waves need to be determined. The previous equation can be expressed as

$$\begin{bmatrix} A_{n,1} \\ A_{n,2} \\ A_{n,3} \\ A_{n,4} \end{bmatrix} = M \begin{bmatrix} A_{1,1} \\ A_{1,2} \\ A_{1,3} \\ A_{1,4} \end{bmatrix}.$$

According to the convention established in the previous section, the applied waves $A_{1,1}$, $A_{1,3}$, $A_{n,2}$, and $A_{n,4}$ are known while the outgoing waves $A_{1,2}$, $A_{1,4}$, $A_{n,1}$, and $A_{n,3}$ are not. By reorganizing the system of equations, it is straightforward to demonstrate that

$$\begin{bmatrix} A_{1,2} \\ A_{1,4} \\ A_{n,1} \\ A_{n,3} \end{bmatrix} = S \begin{bmatrix} A_{1,1} \\ A_{1,3} \\ A_{n,2} \\ A_{n,4} \end{bmatrix}, \tag{7}$$

where

$$S = -\begin{bmatrix} M_{12} & M_{14} & -1 & 0 \\ M_{22} & M_{24} & 0 & 0 \\ M_{32} & M_{34} & 0 & -1 \\ M_{42} & M_{44} & 0 & 0 \end{bmatrix}^{-1} \begin{bmatrix} M_{11} & M_{13} & 0 & 0 \\ M_{21} & M_{23} & -1 & 0 \\ M_{31} & M_{33} & 0 & 0 \\ M_{41} & M_{43} & 0 & -1 \end{bmatrix} \tag{8}$$

is the scattering matrix.

The elements of the scattering matrix can be seen as reflection and transmission coefficients. For general bi-anisotropic material, it is impossible to get a single value for the transmission and the reflection since both of them can occur in two modes.

Note that the scattering matrix (8) relates the amplitudes of modes defined by their tangential components. This is different from the amplitudes determined by many simulation software or experimentally, which usually include out-of-plane components as well. The full modes can be calculated using Eq. (A6) and the scattering matrix renormalized accordingly.

We now have all the tools to calculate the fields at every position in the system. First, the modes and propagation constants are determined for all layers and the transfer matrix of the whole system is calculated, followed by the scattering matrix. Then, the outgoing waves are calculated, giving $\boldsymbol{A}$ in both the input and output media. Finally, $\boldsymbol{A}$ is calculated in every layer by recursive application of transfer matrices from either the input or the output media. We use these values in the next section to calculate the nonlinear effects.

III. NONLINEAR TRANSFER MATRIX APPROACH

In the previous section, we established how to calculate the fields inside a stack of bianisotropic linear materials. In this section, we extend the analysis to nonlinear effects. Our approach generalizes that of Bethune [16,17], who only considered the case of a simply anisotropic material with electric nonlinearity.

As is customary, we assume that the material nonlinearity can be described using a power series expansion. For simplicity, let us consider a second-order process, sum frequency generation (SFG). In SFG, the interaction of two applied waves at ω_1 and ω_2 produces a wave at $\omega_3 = \omega_1 + \omega_2$. This case can easily be generalized to difference frequency generation by changing the signs of the frequency and the propagation vectors at either ω_1 or ω_2, and to second harmonic generation (SHG) by considering $\omega_1 = \omega_2$.

In homogeneous materials, only electric nonlinearities are typically present. However, in metamaterials, magnetic and magnetoelectric nonlinearities are often present, and dominate in many geometries. It is even quite frequent to have multiple nonlinearities present in the same metamaterial and they must therefore all be considered at once.

To represent all possible quadratic nonlinear effects, we use the notation $\chi^{(2)}_{abc,\alpha\beta\gamma}$ where a, b, and c can each take the values e or m while α, β, and γ can each take the values x, y, or z. The first pair of indices, a and α, represent the nature (electric or magnetic) and orientation of the field at the sum frequency ω_3, while the two other pairs indicate the same properties for the two applied waves at ω_1 and ω_2. For example, $\chi^{(2)}_{\mathrm{emm},xyy}$ indicates how the y component of the magnetic fields at ω_1 and ω_2 interact to create a nonlinear polarization in

the x axis. Considering the electric or magnetic nature of the phenomenon at all three frequencies involved, and the three space dimensions, there are a total of $2^3 3^3 = 216$ terms in the second-order susceptibility tensors.

We assume that the nonlinear process is weak enough that it does not significantly affect the amplitude of the applied waves. This is known as the nondepleted pump approximation, and is valid in many practical applications of nonlinear materials. In the particular case of retrieval, which is our main interest here, it is always possible to control the amplitude of the applied waves such that the approximation is respected. With this approximation, the nonlinear wave can be calculated by following a series of simple steps: (1) determine the amplitude of the electric and magnetic fields at ω_1 and ω_2 at all positions inside the stack using the linear transfer matrix approach described in previous sections; (2) calculate the nonlinear polarization and magnetization, and bound waves at ω_3; and (3) couple bound waves to propagating waves at ω_3. We now show how to perform steps 2 and 3.

A. Nonlinear polarization and magnetization, and bound waves

The interaction between waves at ω_1 and ω_2 propagating with $\boldsymbol{k}(\omega_1)$ and $\boldsymbol{k}(\omega_2)$ creates nonlinear polarization and magnetization at $\boldsymbol{k}^{\mathrm{NL}} = \boldsymbol{k}(\omega_1) + \boldsymbol{k}(\omega_2)$. This must be distinguished from normal waves propagating at ω_3 which preserve the in-plane components of the propagation vector according to $k_{x,y}(\omega_3) = k_{x,y}(\omega_1) + k_{x,y}(\omega_2)$, but where the z component must be determined according to the properties of the material with Eq. (1).

Since there are four propagation modes at every frequency, the propagation constants $\boldsymbol{k}(\omega_1)$ and $\boldsymbol{k}(\omega_2)$ can both take four different values, and $\boldsymbol{k}^{\mathrm{NL}}$ can take 16 (possibly degenerate) values. In the nondepleted pump approximation, the different components do not interact. Therefore, they can be calculated separately and then simply summed. At any position in the system, the nonlinear polarization and magnetization for one of those components are

$$\begin{aligned} P^{\mathrm{NL}}_{\boldsymbol{k}^{\mathrm{NL}}_{p,q},\alpha} = \epsilon_0 \sum_{\beta\gamma} & \chi^{(2)}_{\mathrm{eee},\alpha\beta\gamma}(\omega_3;\omega_1,\omega_2) \\ & \times E_{\boldsymbol{k}_{p(\omega_1),\beta}}(\omega_1) E_{\boldsymbol{k}_{q(\omega_2),\gamma}}(\omega_2) \\ & + \chi^{(2)}_{\mathrm{eem},\alpha\beta\gamma}(\omega_3;\omega_1,\omega_2) E_{\boldsymbol{k}_{p(\omega_1),\beta}}(\omega_1) H_{\boldsymbol{k}_{q(\omega_2),\gamma}}(\omega_2) \\ & + \chi^{(2)}_{\mathrm{eme},\alpha\beta\gamma}(\omega_3;\omega_1,\omega_2) H_{\boldsymbol{k}_{p(\omega_1),\beta}}(\omega_1) E_{\boldsymbol{k}_{q(\omega_2),\gamma}}(\omega_2) \\ & + \chi^{(2)}_{\mathrm{emm},\alpha\beta\gamma}(\omega_3;\omega_1,\omega_2) H_{\boldsymbol{k}_{p(\omega_1),\beta}}(\omega_1) H_{\boldsymbol{k}_{q(\omega_2),\gamma}}(\omega_2), \end{aligned} \tag{9a}$$

$$\begin{aligned} M^{\mathrm{NL}}_{\boldsymbol{k}^{\mathrm{NL}}_{p,q},\alpha} = \mu_0 \sum_{\beta\gamma} & \chi^{(2)}_{\mathrm{mee},\alpha\beta\gamma}(\omega_3;\omega_1,\omega_2) \\ & \times E_{\boldsymbol{k}_{p(\omega_1),\beta}}(\omega_1) E_{\boldsymbol{k}_{q(\omega_2),\gamma}}(\omega_2) \\ & + \chi^{(2)}_{\mathrm{mem},\alpha\beta\gamma}(\omega_3;\omega_1,\omega_2) E_{\boldsymbol{k}_{p(\omega_1),\beta}}(\omega_1) H_{\boldsymbol{k}_{q(\omega_2),\gamma}}(\omega_2) \\ & + \chi^{(2)}_{\mathrm{mme},\alpha\beta\gamma}(\omega_3;\omega_1,\omega_2) H_{\boldsymbol{k}_{p(\omega_1),\beta}}(\omega_1) E_{\boldsymbol{k}_{q(\omega_2),\gamma}}(\omega_2) \\ & + \chi^{(2)}_{\mathrm{mmm},\alpha\beta\gamma}(\omega_3;\omega_1,\omega_2) H_{\boldsymbol{k}_{p(\omega_1),\beta}}(\omega_1) H_{\boldsymbol{k}_{q(\omega_2),\gamma}}(\omega_2). \end{aligned} \tag{9b}$$

The indices α, β, and γ take values x, y, and z and indicate the orientation of the fields at ω_3, ω_1, and ω_2, respectively. The indices p and q take values 1–4 and indicate the mode considered at ω_1 and ω_2, respectively.

The nonlinear polarization and magnetization drive bound waves $\boldsymbol{E_s}$ and $\boldsymbol{H_s}$. Their amplitude can be determined by solving the wave equation in the presence of a driving term

$$\begin{aligned} & \begin{bmatrix} [0] & -[\nabla\times] \\ [\nabla\times] & [0] \end{bmatrix}_{\boldsymbol{k}^{\mathrm{NL}}_{p,q}} \begin{bmatrix} \boldsymbol{E_s} \\ \boldsymbol{H_s} \end{bmatrix}_{\boldsymbol{k}^{\mathrm{NL}}_{p,q}} \\ & \quad = i\omega_3 \left(\begin{bmatrix} [\epsilon(\omega_3)] & [\xi(\omega_3)] \\ [\zeta(\omega_3)] & [\mu(\omega_3)] \end{bmatrix} \begin{bmatrix} \boldsymbol{E_s} \\ \boldsymbol{H_s} \end{bmatrix}_{\boldsymbol{k}^{\mathrm{NL}}_{p,q}} + \begin{bmatrix} \boldsymbol{P}^{\mathrm{NL}} \\ \boldsymbol{M}^{\mathrm{NL}} \end{bmatrix}_{\boldsymbol{k}^{\mathrm{NL}}_{p,q}} \right), \end{aligned} \tag{10}$$

where the curl matrix includes the propagation constants used when calculating the nonlinear polarization and magnetization, while the material matrix is calculated at ω_3. Therefore, the bound waves are

$$\begin{aligned} \begin{bmatrix} \boldsymbol{E_s} \\ \boldsymbol{H_s} \end{bmatrix}_{\boldsymbol{k}^{\mathrm{NL}}_{p,q}} = \Bigg(& \frac{-i}{\omega_3} \begin{bmatrix} [0] & -[\nabla\times] \\ [\nabla\times] & [0] \end{bmatrix}_{\boldsymbol{k}^{\mathrm{NL}}_{p,q}} \\ & - \begin{bmatrix} [\epsilon(\omega_3)] & [\xi(\omega_3)] \\ [\zeta(\omega_3)] & [\mu(\omega_3)] \end{bmatrix} \Bigg)^{-1} \begin{bmatrix} \boldsymbol{P}^{\mathrm{NL}} \\ \boldsymbol{M}^{\mathrm{NL}} \end{bmatrix}_{\boldsymbol{k}^{\mathrm{NL}}_{p,q}}. \end{aligned} \tag{11}$$

If the material properties are the same at all frequencies involved (or more precisely if the propagation constants at ω_3 are the sum of the propagation constants at ω_1 and ω_2), the above system of equations is singular. This corresponds to perfect phase matching. This singularity can be removed when the bound waves are included in Eq. (14) below. In a numerical implementation, one can simply impose a small difference in material properties to avoid this issue.

B. Coupling to propagating waves

Now that we have determined the bound waves created by the nonlinear process, we must determine how they couple to propagating waves. In the nondepleted pump approximation, the nonlinearity of each layer can be treated separately and simply summed. As in the linear case, the in-plane components of the waves, now including bound waves, must be continuous at the interface between layers. Therefore, if layer i is nonlinear, at its two interfaces,

$$\Pi_{i-1} A_{i-1}(z_i) = \Pi_i A_i(z_i) + \Pi_s \sum_{p,q} \begin{bmatrix} \boldsymbol{E}_s(z_i) \\ \boldsymbol{H}_s(z_i) \end{bmatrix}_{\boldsymbol{k}^{\mathrm{NL}}_{p,q}}, \tag{12a}$$

$$\Pi_i A_i(z_{i+1}) + \Pi_s \sum_{p,q} \begin{bmatrix} \boldsymbol{E}_s(z_{i+1}) \\ \boldsymbol{H}_s(z_{i+1}) \end{bmatrix}_{\boldsymbol{k}^{\mathrm{NL}}_{p,q}} = \Pi_{i+1} A_{i+1}(z_{i+1}), \tag{12b}$$

where all the transfer matrices are implicitly calculated at ω_3 and

$$\Pi_s = \begin{bmatrix} 1 & 0 & 0 & 0 & 0 & 0 \\ 0 & 0 & 0 & 0 & 1 & 0 \\ 0 & 1 & 0 & 0 & 0 & 0 \\ 0 & 0 & 0 & -1 & 0 & 0 \end{bmatrix}$$

is a matrix that selects the in-plane components of the bound waves. The sum over all p and q accounts for the 16 values of $\boldsymbol{k}_{p,q}^{\mathrm{NL}}$ described above.

Using $A_i(z_{i+1}) = \Phi_i A_i(z_i)$ and

$$\begin{bmatrix} \boldsymbol{E}_s(z_{i+1}) \\ \boldsymbol{H}_s(z_{i+1}) \end{bmatrix}_{\boldsymbol{k}_{p,q}^{\mathrm{NL}}} = \exp\left(ik_{p,q,z}^{\mathrm{NL}} d_i\right) \begin{bmatrix} \boldsymbol{E}_s(z_i) \\ \boldsymbol{H}_s(z_i) \end{bmatrix}_{\boldsymbol{k}_{p,q}^{\mathrm{NL}}},$$

which relate the propagating and bound waves at both ends of the layer, respectively, Eqs. (12) can be combined into

$$\boldsymbol{A}_{i+1} = M_{i,i+1}\Phi_i(M_{i-1,i}\Phi_{i-1}\boldsymbol{A}_{i-1} + \boldsymbol{S}_i), \tag{13}$$

where all the amplitudes vectors are evaluated at the bottom of their respective layers,

$$\boldsymbol{S}_i = \Phi_i^{-1} M_{s,i} \sum_{p,q} \exp\left(ik_{p,q,z}^{\mathrm{NL}} d\right) \begin{bmatrix} \boldsymbol{E}_s \\ \boldsymbol{H}_s \end{bmatrix}_{\boldsymbol{k}_{p,q}^{\mathrm{NL}}} - M_{s,i} \sum_{p,q} \begin{bmatrix} \boldsymbol{E}_s \\ \boldsymbol{H}_s \end{bmatrix}_{\boldsymbol{k}_{p,q}^{\mathrm{NL}}} \tag{14}$$

is the source term representing the nonlinear effect, and $M_{s,i} = \Pi_i^{-1}\Pi_s$. Isolating $\boldsymbol{S}_i$ yields

$$\boldsymbol{S}_i = \Phi_i^{-1} M_{i,i+1}^{-1} \boldsymbol{A}_{i+1} - M_{i-1,i}\Phi_{i-1}\boldsymbol{A}_{i-1}. \tag{15}$$

The amplitude vectors $\boldsymbol{A}_{i+1}$ and $\boldsymbol{A}_{i-1}$ can be connected to the amplitude vectors in the semi-infinite media on either sides of the stack such that

$$R^{-1}\boldsymbol{A}_n - L\boldsymbol{A}_1 = \boldsymbol{S}_i, \tag{16}$$

where

$$L = M_{i-1,i} \ldots \Phi_2 M_{1,2}, \tag{17}$$

$$R = M_{n-1,n}\Phi_n \ldots M_{i,i+1}\Phi_i \tag{18}$$

are the transfer matrices on the left and right of layer i.

Finally, since there is no applied wave at ω_3, only the outgoing waves need to be determined and Eq. (16) simplifies to

$$\begin{bmatrix} A_{1,2} \\ A_{1,4} \\ A_{n,1} \\ A_{n,3} \end{bmatrix} = \left(-L \begin{bmatrix} 0 & 0 \\ 1 & 0 \\ 0 & 0 \\ 0 & 1 \end{bmatrix} - R^{-1} \begin{bmatrix} 1 & 0 \\ 0 & 0 \\ 0 & 1 \\ 0 & 0 \end{bmatrix} \right)^{-1} \boldsymbol{S}_i. \tag{19}$$

In the particular case of a single layer, which is the one appropriate for retrieval, $L = M_{1,2}$ and $R = M_{2,3}\Phi_2$.

IV. RETRIEVAL APPROACH

In the previous section, we showed how to calculate the fields generated by a stack of nonlinear materials. In this section, we present an approach to perform the inverse operation: determine the unknown nonlinear susceptibilities of a slab of material. This approach applies to any nonlinear material, but it is of particular interest for metamaterials, which often are bianisotropic and have more than one nonlinear susceptibility. Our approach generalizes that of Larouche, Rose, and Smith [9], who treated the simpler case of materials with separable nonlinear properties for each axis and polarization.

Looking at Eq. (III A), it is obvious that, while the nonlinear polarization and magnetization depend nonlinearly on the fields, they depend linearly on the nonlinear susceptibilities. This suggests that it is possible to build a linear system of equations to determine the unknown nonlinear susceptibilities. In the case of SFG, there are a total of 216 complex nonlinear susceptibilities. To determine all of them, it is necessary to build a system of 216 complex equations.

This system of equations must be built using nonredundant illumination conditions. Such conditions are obtained by changing the angle of incidence of the applied waves, their polarization, and whether they come from medium 1, medium n, or both. To probe all nonlinearities, it is essential to use applied waves at ω_1 and ω_2 with all possible combinations of polarizations as well as oblique incidence.

Each illumination condition generates four measurements: the amplitude of the two outgoing wave modes in media 1 and n. Therefore, it is necessary to find 54 independent illumination conditions. With these 54 illumination conditions, we build a linear system of equations

$$\begin{bmatrix} A_{1,2}|^{\text{ill. cond. 1}}_{\chi^{(2)}_{\text{eee},xxx}=1} & A_{1,2}|^{\text{ill. cond. 1}}_{\chi^{(2)}_{\text{eee},xxy}=1} & \cdots \\ A_{1,4}|^{\text{ill. cond. 1}}_{\chi^{(2)}_{\text{eee},xxx}=1} & A_{1,2}|^{\text{ill. cond. 1}}_{\chi^{(2)}_{\text{eee},xxy}=1} & \cdots \\ A_{n,1}|^{\text{ill. cond. 1}}_{\chi^{(2)}_{\text{eee},xxx}=1} & A_{1,2}|^{\text{ill. cond. 1}}_{\chi^{(2)}_{\text{eee},xxy}=1} & \cdots \\ A_{n,3}|^{\text{ill. cond. 1}}_{\chi^{(2)}_{\text{eee},xxx}=1} & A_{1,2}|^{\text{ill. cond. 1}}_{\chi^{(2)}_{\text{eee},xxy}=1} & \cdots \\ \vdots & \vdots & \ddots \end{bmatrix} \begin{bmatrix} \chi^{(2)}_{\text{eee},xxx} \\ \chi^{(2)}_{\text{eee},xxy} \\ \vdots \end{bmatrix} = \begin{bmatrix} A_{1,2}|^{\text{ill. cond. 1}}_{\text{expt.}} \\ A_{1,4}|^{\text{ill. cond. 1}}_{\text{expt.}} \\ A_{n,1}|^{\text{ill. cond. 1}}_{\text{expt.}} \\ A_{n,3}|^{\text{ill. cond. 1}}_{\text{expt.}} \\ \vdots \end{bmatrix}, \tag{20}$$

where the matrix contains the outgoing waves at ω_3 calculated using the known linear properties and supposing that each of the 216 nonlinear susceptibilities is separately equal to 1. Each set of four rows corresponds to the four outgoing waves for one illumination condition. Each column corresponds to one nonlinear susceptibility. The vector on the left side contains the unknown nonlinear susceptibilities while the vector on the right contains the amplitude of the outgoing modes measured experimentally or simulated for the same 54 illumination conditions.

To verify that a set of illumination conditions are independent, one can calculate the matrix and verify that it is not singular. To ensure stability of the numerical solution of the linear system of equations, the matrix should also have the smallest possible condition number. In our tests, we have found that using random illumination conditions provides a good condition number. However, such illumination conditions are extremely impractical for experiments, and difficult to implement even for simulations. To simplify the setup of the experiment or simulations, it is possible to limit ourselves to a few angles of incidence, and to TE and TM applied waves.

TABLE I. A set of 54 independent illumination conditions are obtained by taking all combinations of applied modes (top) and of angles of incidence (bottom).

Mode combinations

ω_1				ω_2			
$A_{1,1}$ (V/m)	$A_{1,3}$ (V/m)	$A_{n,2}$ (V/m)	$A_{n,4}$ (V/m)	$A_{1,1}$ (V/m)	$A_{1,3}$ (V/m)	$A_{n,2}$ (V/m)	$A_{n,4}$ (V/m)
1	0	1	0	1	0	1	0
1	0	1	0	0	1	0	1
0	1	0	1	1	0	1	0
0	1	0	1	0	1	0	1
1	0	−1	0	1	0	−1	0
0	1	0	−1	0	1	0	−1

Angle of incidence combinations

ω_1		ω_2	
θ_x (degrees)	θ_y (degrees)	θ_x (degrees)	θ_y (degrees)
0	0	0	0
0	0	0	30
0	0	30	0
0	30	0	0
0	−30	0	−30
0	30	−30	0
30	0	0	0
-30	0	0	30
30	0	30	0

Table I shows one possible set of illumination conditions that was used for the example below.

In summary, to perform retrieval of the nonlinear susceptibilities of a metamaterial, one should (1) determine the linear properties of the metamaterial at all frequencies of interest using linear retrieval approaches [4–6]; (2) perform a series of independent experiments or simulations (54 in the case of SFG), and measure the nonlinearly generated waves in both modes in media 1 and n; (3) build the matrix by performing a series of calculations using the known linear properties and assuming that each nonlinear susceptibility term is independently equal to 1; and (4) solve the linear system of equations created by the matrix of all forward calculations and the measurements.

TABLE II. Normalization values for the various nonlinear susceptibility tensors.

Susceptibility	Normalization
$\chi^{(2)}_{\text{eee}}$	1
$\chi^{(2)}_{\text{eem}}$	Z_0^{-1}
$\chi^{(2)}_{\text{eme}}$	Z_0^{-1}
$\chi^{(2)}_{\text{emm}}$	Z_0^{-2}
$\chi^{(2)}_{\text{mee}}$	Z_0
$\chi^{(2)}_{\text{mem}}$	1
$\chi^{(2)}_{\text{mme}}$	1
$\chi^{(2)}_{\text{mmm}}$	Z_0^{-1}

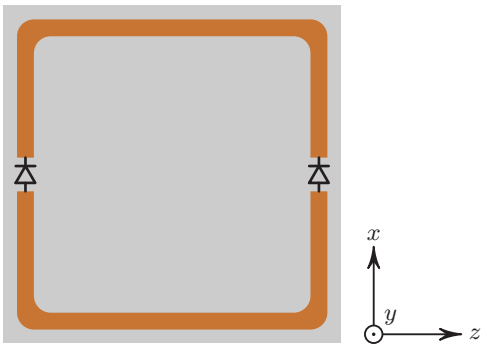

FIG. 2. The VLSRR considered in the example. The unit cell is cubic with a side of 1 cm. The substrate is FR4 with a thickness of 254 μm, covered with 17 μm of copper; the external dimension of the ring is 9.2 mm and its linewidth is 0.5 mm. Varactor diodes are inserted in the 1 mm gaps (see text for details). The propagation direction is z while the metamaterial is considered infinite in the x and y directions.

Stability and validation

For the same numerical value, different types of nonlinearity can produce nonlinear waves whose amplitudes differ by many orders of magnitude. This is due to the difference between the value of the electric and magnetic fields. In vacuum, their ratio is $Z_0 = \sqrt{\mu_0/\epsilon_0} \approx 377\,\Omega$, while it is close to this value for most materials. This can easily make the proposed retrieval method unstable if not accounted for. To counteract this effect, each nonlinear susceptibility can be normalized by dividing it by Z_0 when the magnetic field is considered at ω_1 or ω_2 and by multiplying it by Z_0 when the magnetic field is considered at ω_3. Table II shows the normalization for all nonlinear susceptibility tensors.

To validate the retrieval approach, we first made sure that it gives self-consistent results when applied to nonlinear fields calculated using the transfer matrix approach of Sec. III. Unsurprisingly, in that case, the retrieved nonlinear susceptibilities are within a part in a billion of the imposed values. Then, we applied the retrieval approach to nonlinear simulations performed on uniform slabs of material using COMSOL [18]. In that case, the retrieved values are within a few percent of the

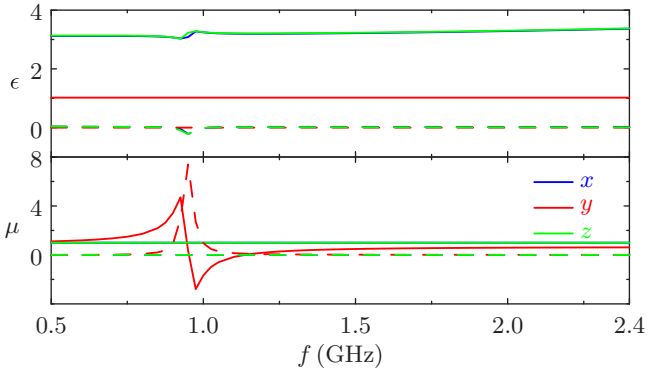

FIG. 3. Linear properties of the VLSRR of Fig. 2. The real part (continuous lines) and imaginary part (dashed lines) of the permittivity (top) and permeability (bottom) are all diagonal.

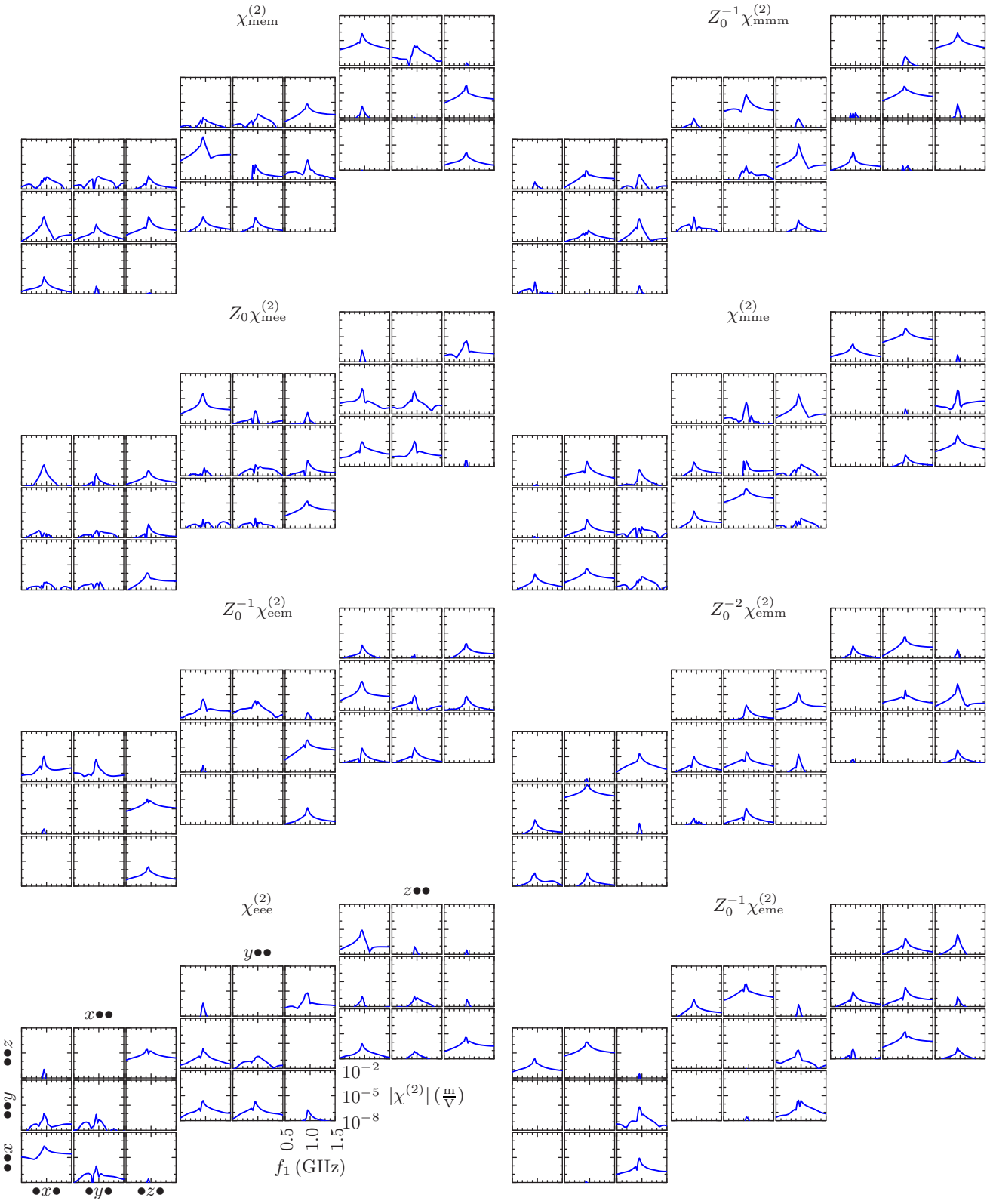

FIG. 4. Norm of the second-order nonlinear susceptibilities of the VLSRR. To put all values on the same scale, nonlinear susceptibilities involving magnetic terms are normalized using the impedance of vacuum Z_0. For each type of nonlinearity, the results are presented in three slices, corresponding to the orientation of the field at f_3. In each slice, columns and rows correspond to the orientation of the fields at f_1 and f_2, respectively. All subplots share the same axes.

imposed values. More details about the validation are provided in Appendix B.

V. EXAMPLE: VARACTOR-LOADED SPLIT RING RESONATOR

Let us now apply the method we propose to the case of the varactor-loaded split-ring resonator (VLSRR). VLSRRs are the canonical example of a nonlinear metamaterial [19,20]. The SRR concentrates electric fields in the small volume of its gaps. If a nonlinear material or component is present in the gap, its nonlinear properties are amplified. We use the VLSRR shown in Fig. 2, which has the same dimensions and material properties as those used in Ref. [9]. Varactors are included in both gaps and they are oriented in the same direction. When the VLSRR is exposed to electromagnetic waves, the varactors naturally reverse bias. They can therefore be simulated using a simplified model consisting of a 2.35 pF capacitor in series with a 2.5 Ω resistor.

The electromagnetic response of the VLSRR was simulated using COMSOL [18]. First, a series of time-harmonic linear simulations were performed illuminating the SRR from various directions and with various polarizations. The standard linear retrieval approach was used to determine the linear properties, shown in Fig. 3. As expected, the dominant response of the SRR is a magnetic resonance in the y axis, which occurs around 0.9 GHz. There is no magnetic response in the two other axes. The SRR also has a nonresonant electric response for fields polarized in the plane of the SRR.

Next, the 54 nonlinear simulations described in Table I were performed to determine the outgoing fields at frequency $f_3 = \omega_3/2\pi$. In those simulations, we varied $f_1 = \omega_1/2\pi$ between 0.5 and 1.5 GHz, while $f_2 = \omega_2/2\pi$ was kept constant at 0.9 GHz. The simulations involved three time-harmonic simulations at the three frequencies involved. At each frequency, two circuit models, one for each varactor, were connected inside of the gaps. The nonlinear coupling between the three frequencies occurs in the varactor, whose capacitance is nonlinear. To account for this, we assume that the potentials on the capacitor at f_1 and f_2, V_1 and V_2, generate a potential at f_3 given by $V_3 = a_2 V_1 V_2$ where $a_2 = 0.2667\ \mathrm{V}^{-1}$ comes from a power series expansion of the varactor capacitance [21].

We then used MATLAB [22] to generate the retrieval matrix, and solve the linear system of equations to retrieve all 216 nonlinear susceptibility terms shown in Fig. 4. We determined the complex values for the nonlinear susceptibilities, but for simplicity only show their norm. The range of simulations we performed includes second harmonic generation ($f_1 = f_2 = 0.9$ GHz). In that case, the fields at f_1 and f_2 are indistinguishable; to avoid an underdetermined system of equations, we assumed that $\chi^{(2)}_{abc,\alpha\beta\gamma} = \chi^{(2)}_{acb,\alpha\gamma\beta}$.

The main result that can be observed in Fig. 4 is that $\chi^{(2)}_{\mathrm{emm},xyy}$ is about one order of magnitude larger than any other term. This is not surprising; the applied waves at f_1 and f_2 are both close to the magnetic resonance frequency of the element, such that a magnetic field in the y axis couples well in the VLSRR. Since the two diodes are oriented in the same direction, they generate potentials at f_3 that are also in the same direction. This symmetry corresponds to that of an electric field in the x axis.

The term $\chi^{(2)}_{\mathrm{eee},xxx}$ is also supported by the geometry. Electric fields oriented along the x axis at f_1 and f_2 polarize the two varactors, which generate an electric field in the x direction at f_3. However, when the VLSRR is excited by an electric field, most of field concentrates between adjacent rings, rather than in the gaps, such that this nonlinearity is significantly smaller than $\chi^{(2)}_{\mathrm{emm},xyy}$. Similar arguments can be made for the terms $\chi^{(2)}_{\mathrm{eem},xxy}$ and $\chi^{(2)}_{\mathrm{eme},xyx}$.

The retrieval indicates that many other nonlinearities are present which do not seem to be supported by the geometry. They can all be explained by spatial dispersion [10,23]. Spatial dispersion occurs because the metamaterial elements, which are discrete, are replaced by a homogeneous layer of finite thickness where the nonlinearity is distributed. The magnitude of this effect is related to the ratio between the size of the unit cell and all the wavelengths involved. At the resonance frequency, the refractive index of the VLSRR is maximum with a value of about four. The wavelength inside of the metamaterial is about 8 cm, less than an order of magnitude larger than the unit cell. Therefore, spatial dispersion shows mainly at that frequency.

It is fairly easy to understand the significant nonlinear susceptibilities of the VLSRR because the axes of the chosen system of coordinates correspond to symmetries of the unit cell. Such a choice is often natural for the simulation or characterization of metamaterials. However, the proposed approach works for an arbitrary choice of coordinate system. The effective properties in various coordinate systems are related through standard tensor transformation laws.

VI. CONCLUSION

We have proposed a nonlinear transfer matrix appropriate for bianisotropic materials with any combination of nonlinearities and showed how this approach can be used to retrieve the effective nonlinear susceptibilities of a metamaterial.

For simplicity, we have demonstrated the approach using SFG, a second-order process. However, our approach generalizes easily to a process of any order, with a rapidly increasing number of terms. In general, for an nth-order process, there are 2^{n+1} nonlinear susceptibility tensors, each containing 3^{n+1} terms, for a total of 6^{n+1} independent terms. For a third-order process, for example, there are 1296 elements.

The proposed approach works for 3D metamaterials where it is possible to define layers with finite thicknesses inside which waves propagate according to the modes described in this paper. It is not directly applicable to metasurfaces; however, a retrieval method already exists for anisotropic nonlinear metasurfaces [24].

We hope that the application of our method will encourage the development of complex nonlinear metamaterials with many nonlinear susceptibilities enabling new exciting applications.

ACKNOWLEDGMENT

This work was approved for public release under Release No. NG18-0699.

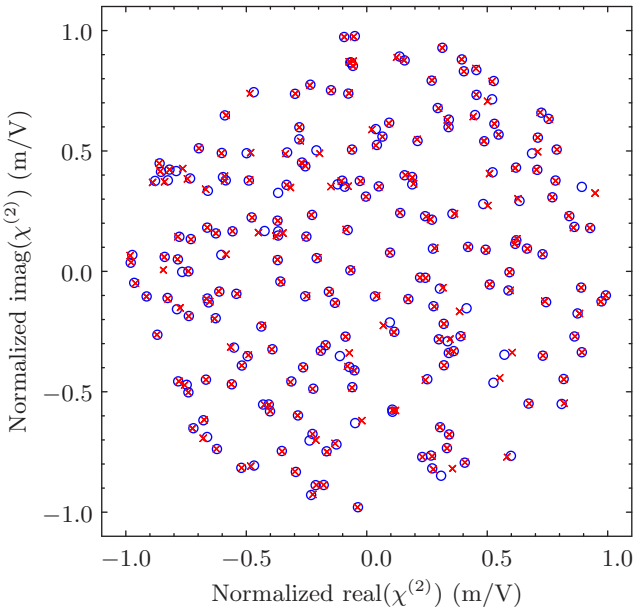

FIG. 5. Typical retrieval validation results for a material with the linear properties presented in Table III and randomly selected nonlinear susceptibility tensors. Circles represent the normalized nonlinear susceptibilities imposed in the simulation, while crosses represent the normalized nonlinear susceptibilities retrieved from the simulation results. Each pair of a circle and a cross represents one of the 216 nonlinear susceptibilities. The retrieval would be perfect if all pairs overlapped.

APPENDIX A: PROPAGATION MODES IN BIANISOTROPIC LINEAR MATERIALS

In this appendix, we review Berreman's approach to find the propagation modes in a slab of anisotropic, bianisotropic, and/or magnetoelectric material [14]. In the absence of free charges and currents, Maxwell's curl equations in the frequency domain ($e^{-i\omega t}$ time convention, where ω is the angular frequency and t the time) are

$$\nabla \times \boldsymbol{E} = i\omega \boldsymbol{B}, \tag{A1a}$$

$$-\nabla \times \boldsymbol{H} = i\omega \boldsymbol{D}, \tag{A1b}$$

where $\boldsymbol{E}$ and $\boldsymbol{H}$ are the electric and magnetic fields, $\boldsymbol{B}$ is the magnetic induction, and $\boldsymbol{D}$ is the electric displacement. The material equations are

$$\boldsymbol{D} = \epsilon \boldsymbol{E} + \xi \boldsymbol{H}, \tag{A2a}$$

$$\boldsymbol{B} = \zeta \boldsymbol{E} + \mu \boldsymbol{H}, \tag{A2b}$$

where ϵ and μ are the permittivity and the permeability, while ξ and ζ are the magnetoelectric coupling coefficients. All the material properties are 3×3 rank-two tensors.

Maxwell's equations and the material equations can be combined in a single matrix equation

$$\begin{bmatrix} [0] & -[\nabla\times] \\ [\nabla\times] & [0] \end{bmatrix} \begin{bmatrix} \boldsymbol{E} \\ \boldsymbol{H} \end{bmatrix} = i\omega \begin{bmatrix} [\epsilon] & [\xi] \\ [\zeta] & [\mu] \end{bmatrix} \begin{bmatrix} \boldsymbol{E} \\ \boldsymbol{H} \end{bmatrix}, \tag{A3}$$

where [0] is a 3×3 null matrix and

$$[\nabla\times] = \begin{bmatrix} 0 & -\frac{\partial}{\partial z} & \frac{\partial}{\partial y} \\ \frac{\partial}{\partial z} & 0 & -\frac{\partial}{\partial x} \\ -\frac{\partial}{\partial y} & \frac{\partial}{\partial x} & 0 \end{bmatrix}.$$

Inside a uniform medium, this equation is a first-order wave equation with solutions of the form

$$\begin{bmatrix} \boldsymbol{E}(x,y,z) \\ \boldsymbol{H}(x,y,z) \end{bmatrix} = \exp[i(k_x x + k_y y + k_z z)] \begin{bmatrix} \boldsymbol{E}(0) \\ \boldsymbol{H}(0) \end{bmatrix}, \tag{A4}$$

where k_x, k_y, and k_z are the components of the propagation constant. Therefore, the partial derivatives $\frac{\partial}{\partial x,y,z}$ can be replaced by $ik_{x,y,z}$ and the curl operator by

$$[\nabla\times] = \begin{bmatrix} 0 & -ik_z & ik_y \\ ik_z & 0 & -ik_x \\ -ik_y & ik_x & 0 \end{bmatrix}.$$

The third and sixth rows of Eq. (A3) are

$$\begin{bmatrix} 0 & 0 & 0 & ik_y & -ik_x & 0 \\ -ik_y & ik_x & 0 & 0 & 0 & 0 \end{bmatrix} \begin{bmatrix} \boldsymbol{E} \\ \boldsymbol{H} \end{bmatrix} = i\omega \begin{bmatrix} \epsilon_{zx} & \epsilon_{zy} & \epsilon_{zz} & \xi_{zx} & \xi_{zy} & \xi_{zz} \\ \zeta_{zx} & \zeta_{zy} & \zeta_{zz} & \mu_{zx} & \mu_{zy} & \mu_{zz} \end{bmatrix} \begin{bmatrix} \boldsymbol{E} \\ \boldsymbol{H} \end{bmatrix}. \tag{A5}$$

Since k_x, k_y, and the material properties are known, these two equations relate the components of the fields. They can be used to express two field components as a function of the four others. Since our goal is to develop an approach for multilayer stacks, it is obviously advantageous to work with the components of the fields that are continuous at the interface between the layers, namely, E_x, E_y, H_x, and H_y, while E_z and H_z are eliminated. The z components of the fields are

$$\begin{bmatrix} E_z \\ H_z \end{bmatrix} = -\begin{bmatrix} \epsilon_{zz} & \xi_{zz} \\ \zeta_{zz} & \mu_{zz} \end{bmatrix}^{-1} \times \begin{bmatrix} \epsilon_{zx} & \epsilon_{zy} & \xi_{zx} - \frac{k_y}{\omega} & \xi_{zy} + \frac{k_x}{\omega} \\ \zeta_{zx} + \frac{k_y}{\omega} & \zeta_{zy} - \frac{k_x}{\omega} & \mu_{zx} & \mu_{zy} \end{bmatrix} \begin{bmatrix} E_x \\ E_y \\ H_x \\ H_y \end{bmatrix}. \tag{A6}$$

Separating the z components in the four remaining equations yields

$$\begin{bmatrix} 0 & 0 & 0 & ik_z \\ 0 & 0 & -ik_z & 0 \\ 0 & -ik_z & 0 & 0 \\ ik_z & 0 & 0 & 0 \end{bmatrix} \begin{bmatrix} E_x \\ E_y \\ H_x \\ H_y \end{bmatrix} + \begin{bmatrix} 0 & -ik_y \\ 0 & ik_x \\ ik_y & 0 \\ -ik_x & 0 \end{bmatrix} \begin{bmatrix} E_z \\ H_z \end{bmatrix} = i\omega \left(\begin{bmatrix} \epsilon_{xx} & \epsilon_{xy} & \xi_{xx} & \xi_{xy} \\ \epsilon_{yx} & \epsilon_{yy} & \xi_{yx} & \xi_{yy} \\ \zeta_{xx} & \zeta_{xy} & \mu_{xx} & \mu_{xy} \\ \zeta_{yx} & \zeta_{yy} & \mu_{yx} & \mu_{yy} \end{bmatrix} \begin{bmatrix} E_x \\ E_y \\ H_x \\ H_y \end{bmatrix} + \begin{bmatrix} \epsilon_{xz} & \xi_{xz} \\ \epsilon_{yz} & \xi_{yz} \\ \zeta_{xz} & \mu_{xz} \\ \zeta_{yz} & \mu_{yz} \end{bmatrix} \begin{bmatrix} E_z \\ H_z \end{bmatrix} \right).$$

TABLE III. Linear properties used for the validation retrieval shown in Fig. 5.

f (GHz)	ϵ_{xx}	μ_{xx} and μ_{zz}	Other properties
10	$2.25 + 0.010i$	1.0	1
13	$2.56 + 0.012i$	1.1	1
23	$2.89 + 0.015i$	1.2	1

Moving all z components to the right side, inserting the solution from Eq. (A6), eliminating the matrix on the left side, reordering the rows, and taking the inverse of H_x (to make its value positive for forward propagation in a right-handed material), we obtain Eq. (1).

APPENDIX B: VALIDATION

To validate the proposed nonlinear retrieval approach, we applied it to many sum frequency generation simulation results for uniform slabs of material with known nonlinear susceptibilities. For each case, the 54 nonlinear simulations described in Table I were performed using coupled time-harmonic simulations at f_1, f_2, and f_3 in COMSOL [18]. At the sum frequency f_3, the nonlinear effects were implemented using weak contributions. Since the nondepleted approximation is considered, the nonlinear contributions at f_1 and f_2 are assumed to be negligible.

We ran simulations for a few combinations of frequencies and linear properties, and for many randomly selected complex nonlinear susceptibility tensors. The known nonlinear susceptibilities were selected such that their normalized values fall inside the unit circle. Each value is normalized as described in Sec. IV in order for the nonlinear effect produced to be on the same scale.

Typical validation results are shown in Fig 5. The results are obtained for $f_1 = 10$ GHz, $f_2 = 13$ GHz, and $f_3 = f_1 + f_2 = 23$ GHz. The linear properties are shown in Table III. As can be seen, all normalized retrieved susceptibilities are within a circle of 0.08 m/V of the imposed values, with most of them within 0.01 m/V.

[1] *Nonlinear, Tunable, and Active Metamaterials*, edited by I. V. Shadrivov, M. Lapine, and Y. S. Kivshar (Springer, Switzerland, 2015).

[2] N. I. Zheludev and Y. S. Kivshar, Nat. Mater. **11**, 917 (2012).

[3] A. M. Urbas, Z. Jacob, L. D. Negro, N. Engheta, D. Boardman, P. Egan, A. B. Khanikaev, V. Menon, M. Ferrera, N. Kinsey *et al.*, J. Opt. **18**, 093005 (2016).

[4] D. R. Smith, S. Schultz, P. Markoš, and C. M. Soukoulis, Phys. Rev. B **65**, 195104 (2002).

[5] X. Chen, T. M. Grzegorczyk, B.-I. Wu, J. Pacheco, Jr., and J. A. Kong, Phys. Rev. E **70**, 016608 (2004).

[6] X. Chen, B.-I. Wu, J. A. Kong, and T. M. Grzegorczyk, Phys. Rev. E **71**, 046610 (2005).

[7] S. Larouche and D. R. Smith, Opt. Commun. **283**, 1621 (2010).

[8] A. Rose, S. Larouche, D. Huang, E. Poutrina, and D. R. Smith, Phys. Rev. E **82**, 036608 (2010).

[9] S. Larouche, A. Rose, and D. R. Smith, in *Nonlinear, Tunable, and Active Metamaterials*, Vol. 200, edited by I. V. Shadrivov, M. Lapine, and Y. S. Kivshar (Springer, Switzerland, 2015), Chap. 1, pp. 1–19.

[10] M. A. Gorlach, T. A. Voytova, M. Lapine, Y. S. Kivshar, and P. A. Belov, Phys. Rev. B **93**, 165125 (2016).

[11] Z.-Y. Wang, J.-P. Qiu, H. Chen, J.-J. Mo, and F.-X. Yu, Chin. Phys. B **26**, 094207 (2017).

[12] D. C. Hooper, A. G. Mark, C. Kuppe, J. T. Collins, P. Fischer, and V. K. Valev, Adv. Mater. **29**, 1605110 (2017).

[13] M. Born and E. Wolf, *Principles of Optics*, 7th ed. (Cambridge University Press, Cambridge, UK, 1999).

[14] D. W. Berreman, J. Opt. Soc. Am. **62**, 502 (1972).

[15] P. Yeh, J. Opt. Soc. Am. **69**, 742 (1979).

[16] D. S. Bethune, J. Opt. Soc. Am. B **6**, 910 (1989).

[17] D. S. Bethune, J. Opt. Soc. Am. B **8**, 367 (1991).

[18] COMSOL 5.2a, http://www.comsol.com/.

[19] I. V. Shadrivov, A. B. Kozyrev, D. W. van der Weide, and Y. S. Kivsha, Opt. Express **16**, 20266 (2008).

[20] B. Wang, J. Zhou, T. Koschny, and C. M. Soukoulis, Opt. Express **16**, 16058 (2008).

[21] E. Poutrina, D. Huang, and D. R. Smith, New J. Phys. **12**, 093010 (2010).

[22] MATLAB 2016b, http://www.mathworks.com.

[23] A. Rose, S. Larouche, E. Poutrina, and D. R. Smith, Phys. Rev. A **86**, 033816 (2012).

[24] X. Liu, S. Larouche, and D. R. Smith, Opt. Commun. **410**, 53 (2018).